

Anisotropy of Resonant Inelastic X-Ray Scattering at the K Edge of Si: Theoretical Analysis

Yunori NISIKAWA*, Manabu USUDA, and Jun-ichi IGARASHI†

*Synchrotron Radiation Research Center, Japan Atomic Energy Research Institute, Mikazuki, Sayo,
Hyogo 679-5148*

(Received January 28, 2020)

We investigate theoretically the resonant inelastic x-ray scattering (RIXS) at the K edge of Si with varying transferred-momenta, incident-photon energy and incident-photon polarization. We confirm theoretically the anisotropy of a RIXS and provide a quantitative explanation of a experiment on RIXS at the K edge of Si (Y. Ma *et al.*, Phys. Rev. Lett. 74, 478 (1995)). We clarify the implication of the spectral shape.

KEYWORDS: resonant inelastic X-ray scattering, K edge of Si, anisotropy

1. Introduction

Inelastic x-ray scattering is a promising method to study electronic structures in matters. It is advantageous to use a resonant enhancement by tuning photon energy near absorption edge. Recently it has been revealed that this resonant inelastic x-ray scattering (RIXS) is a powerful tool for elucidating the electronic structures of solids. RIXS measurement has been applied to search for charge excitation modes in several cuprates^{1,2} and manganites,³ with the incident photon energy tuned to the absorption K edge. Since corresponding photon energies are in the hard-X-ray region, the momentum transfer can not be neglected. One of the most interesting subjects is to investigate transferred-momentum dependence of the RIXS spectra.

In our previous paper, we have carried out a RIXS experiment at the K edge of Ge, with systematically varying transferred-momenta and have analyzed the experimental data on the basis of the band structure calculation.⁴ The calculation has reproduced well the experimental data. Against our expectation, we have obtained a broad inelastic peak as a function of photon energy, whose shape is nearly independent of transferred-momenta. Here, we explain briefly the reason why the spectra are nearly independent of final-state momenta. The final state consists of one electron in the conduction band and one hole in the valence band. If the core-hole level in the intermediate state is sharp enough, we can select the momentum of the excited electron in the conduction band by sharply tuning the incident-photon energy. Then, selecting the final-state momentum by setting the scattering geometry, we can specify the momentum of the hole in the valence band. In this situation, one expects sharp peaks at the energy of the

*E-mail address:nisikawa@spring8.or.jp

†Present address:Faculty of Science, Ibaraki University, 2-1-1 Bunkyo, Mito, Ibaraki 310-8512

electron-hole pair, as a function of photon energy. For example, Ma has proposed the idea of valence band structure determination from RIXS spectra by means of scanning scattering vector without changing the incident-photon energy.⁵ We have calculate the RIXS spectra at the K edge of Ge with varying values of the core-level width, to examine a possibility of determining band structure from RIXS experiment. For smaller values of core-level widths, it has been found that we can trace the energy dispersion with varying transfered-momenta. On the other hand, if the core-hole level is as broad as width of conduction band, many channels are opened to excite an electron with different momenta in the conduction band. Therefore, we need to sum up each contribution. In this case, the spectra are approximately given by a superposition of the p -electron density of states(p -DOS). The situation mentioned above is just applied to the RIXS at the K edge of Ge, because the $1s$ core-level width of Ge is estimated about 2eV, which is nearly equal to the width of conduction band of Ge. Therefore, we can naturally explain why the RIXS spectra at the K edge of Ge are nearly independent of transfered-momenta.

On the other hand, the $1s$ core-level width of Si is estimated about 0.6 eV which is smaller than the width of conduction band of Si. The K edge energy of Si is around 1840 eV. So, it is considered that the magnitude of transfered-momentum is not negligible in the RIXS at the K edge of Si. It implies that there is a possibility that the RIXS spectra at the K edge of Si have the transfered-momentum dependence. Actually, according to experiment results obtained by Ma *et. al*, RIXS spectra at the K edge of Si have transfered-momentum dependence.⁶ In this paper, we investigate theoretically the RIXS at the K edge of Si and clarify the implication of the spectral shape, by means of the band structure calculation.

This paper is organized as follows. The formalism for calculating the spectra is described in §2. In §3, the calculated results and discussion are presented. Section 4 is devoted to concluding remarks.

2. Formulation

2.1 Double Differential Scattering Cross-Section

RIXS is described by a second-order process. To obtain the double differential scattering cross-section, we use the generalized Fermi's golden rule where the interaction between light and electrons is treated by second order perturbation theory. For Si, an independent particle treatment for electron system seems to be appropriate, since electron correlations are weak.⁵ Finally, we obtain the double differential scattering cross-section as follows.

$$\frac{d^2\sigma}{d\omega_2 d\Omega_2} \propto \sum_{(\mathbf{k},e),(\mathbf{k}',h)} \frac{\left| \sum_a \exp(i\mathbf{\Omega} \cdot \mathbf{R}_a) \overline{t_a(\mathbf{k}', h|\mathbf{e}_2)} t_a(\mathbf{k}, e|\mathbf{e}_1) \right|^2}{(\epsilon_e(\mathbf{k}) - \epsilon_c - \hbar\omega_1)^2 + \Gamma^2/4} \delta_{\mathbf{\Omega}, \mathbf{k}-\mathbf{k}'}^{\mathbf{G}} \delta(\epsilon_e(\mathbf{k}) - \epsilon_h(\mathbf{k}') - \hbar\omega), \quad (1)$$

where $\hbar\omega = \hbar\omega_1 - \hbar\omega_2$, and $\hbar\mathbf{\Omega} = \hbar\mathbf{q}_1 - \hbar\mathbf{q}_2$ are energy and momentum of the final state and \mathbf{e}_i , $\hbar\omega_i$ and $\hbar\mathbf{q}_i$ denote the polarization vector, the energy and the momentum vector of the incident ($i = 1$) and emitted ($i = 2$) photon, respectively. $\epsilon_e(\mathbf{k})$, $\epsilon_h(\mathbf{k}')$ and ϵ_c are the energy of the excited electron with crystal momentum \mathbf{k} in the conduction band e , that of the hole with crystal momentum \mathbf{k}' in the valence band h , and that of the core state, respectively. The Γ is the $1s$ core-level width of Si. The crystal momentum conservation for the whole process is contained in the factor of Kronecker δ ,

$$\delta_{\mathbf{\Omega}, \mathbf{k}-\mathbf{k}'}^{\mathbf{G}} \equiv \begin{cases} 0 & : \mathbf{\Omega} - (\mathbf{k} - \mathbf{k}') \notin \mathbf{G} \\ 1 & : \mathbf{\Omega} - (\mathbf{k} - \mathbf{k}') \in \mathbf{G} \end{cases}, \quad (2)$$

where \mathbf{G} is the set of reciprocal lattice vectors. Overlined quantities indicate their complex conjugates. By using the dipole approximation, $t_a(\mathbf{p}, \tau | \mathbf{e}) = \int d\mathbf{r} \overline{\psi_{\mathbf{p}, \tau}(\mathbf{r})} \mathbf{e} \cdot \hat{\mathbf{p}} \phi_a^{1s}(\mathbf{r} - \mathbf{R}_a)$, where \mathbf{R}_a , $\psi_{\mathbf{p}, \tau}$ and ϕ_a^{1s} are the position vector of atom a in unit cell, Bloch-wave function of an electron in the τ -band with crystal momentum \mathbf{p} , and $1s$ -atomic orbital, respectively. These quantities are evaluated on the basis of the band structure calculation described in the following sub-section.

2.2 Band Structure Calculation of Si

We calculate the band structure of Si by using the full-potential linearized augmented-plane-wave (FLAPW) method within the local-density approximation (LDA). The local exchange-correlation functional of Vosko *et al.* is employed.⁷ The angular momentum in the spherical-wave expansion is truncated at $l_{\max} = 6$ and 7 for the potential and wave function, respectively. The energy cutoff of the plane wave is 12 Ry for the wave function. Figure 1 shows the energy vs. momentum relation thus evaluated. The energy band is labeled by attached numbers for later use.

3. Calculated Results and Discussion

3.1 RIXS spectra

In our formulation, the input parameters are Γ and ϵ_c . We set $\Gamma = 0.6$ eV^{8,9} and $\epsilon_c = -1839.95$ eV so as to reproduce the absorption coefficient at the K edge (the energy is measured from Fermi level E_F defined in figure 1). In our calculation of RIXS spectra, geometrical relations between \mathbf{q}_1 , \mathbf{q}_2 and crystal axis of Si are assumed as shown in a figure 2. The normal axis \mathbf{n} and theta axis \mathbf{t} in this figure are respectively defined as follows: $\mathbf{n} \propto \mathbf{q}_2 / |\mathbf{q}_2| - \mathbf{q}_1 / |\mathbf{q}_1|$, $\mathbf{t} \propto \mathbf{q}_1 \times \mathbf{q}_2$. The setup for scattering is uniquely determined by choosing the normal and theta axis from crystal axes of Si. We can reproduce the experimental setup of Ma *et al.*⁶ by choosing \mathbf{n} from crystal axes of Si: (111), (110), and (100), and determining appropriate \mathbf{t} . (The theta axis and incident-photon polarization in Ma *et al.*'s experiment are not indicated clearly in their paper.⁶)

3.1.1 Anisotropy of the RIXS at K edge of Si

We investigate the transferred-momentum dependence of RIXS spectra by varying the normal axis \mathbf{n} . Figure 3 shows calculated RIXS spectra for $\hbar\omega_1 = 1840.8$ eV, $\mathbf{n}=(111),(110)$, and (100) in comparison with experimental results by Ma *et. al.*⁶ The calculation reproduces well the experimental shape and feature such as three peak structure in the RIXS spectra for $\mathbf{n} = (111)$. The spectral shape changes with varying \mathbf{n} . Therefore, we confirm theoretically that there exists an anisotropy of RIXS at the K Edge of Si. We clarify the implication of the spectral shape in subsection 3.2.

3.1.2 Incident-photon energy dependence of RIXS spectra

We investigate the incident-photon energy dependence of RIXS spectra. Figure 4 shows calculated RIXS spectra for $\mathbf{n}=(111)$ with varying incident-photon energy between 1840.0 eV and 1841.2 eV. From figure 4, it is found that the characteristic three peaks A, B and C in RIXS spectra for $\mathbf{n} = (111)$ is found only in the narrow energy region between 1840.2 eV and 1840.8 eV. The anisotropy of RIXS almost disappear from the spectra for $\hbar\omega_1 = 1842.5$ eV, as shown in figure 5. The result is consistent with experimental results obtained by Ma *et. al.*⁶

3.1.3 Incident-photon polarization and azimuth angle dependence of RIXS spectra

We investigate incident-photon polarization dependence of RIXS spectra. Figure 6 shows calculated RIXS spectra with varying incident-photon polarization. From figure 6, we can see following facts. The RIXS spectra for $\mathbf{n}=(111)$ and (110) almost have no dependence of incident-photon polarization. On the other hand, the RIXS spectra for $\mathbf{n}=(100)$ change their low energy-loss parts by varying the incident-photon polarization. We also investigate azimuth angle dependence of RIXS spectra for $\mathbf{n}=(111),(110)$ and (100) with varying incident-photon energy between 1840.0 eV and 1841.0 eV. The spectral shapes do not change significantly with varying azimuth angle (whose results are not presented in this paper).

3.2 Clarifying the implication of the spectral shape

Here, we clarify the implication of the spectral shape. The spectra are decomposed into each contribution of band-to-band transitions specified by band indices. Figure 7 shows the result for $\hbar\omega_1 = 1840.8$ eV, $\mathbf{n}=(111)$, (110), and (100). From figure 7, we can see following facts. The three peaks A, B and C of RIXS spectrum for $\mathbf{n}=(111)$ are mainly composed of transitions from the bands 4, 3 and 2 to the band 5, respectively. The maximum peaks of RIXS spectra for $\mathbf{n}=(110)$ and (100) are mainly composed of transitions from the bands 3 and 4 to the band 5. Next, we consider the origin of anisotropy of RIXS at K edge of Si. In our previous study,⁴ we have shown following facts. If the value of core-level width Γ is small enough, spectral components of band-to-band transitions are sharp enough to exist

separately in RIXS spectra. Then, the peaks in a RIXS spectrum correspond to the peaks of spectral components of band-to-band transitions, directly. The Raman-shift of the peak of spectral components corresponding to transition from valence band h to conduction band c is the energy of valence band h measured from minimum energy of conduction band c . Each peak moves directly reflecting dispersion of valence band with varying transferred-momenta. Therefore, RIXS spectra for sufficiently small value of Γ can have the anisotropy and we can trace the valence band structure from the peak position of RIXS spectra by means of scanning transferred-momenta. Here, we compare the RIXS spectra for realistic value of Γ (=0.6 eV) with the RIXS spectra for sufficiently small value of Γ (=0.02 eV) to investigate the relation of the peak position of RIXS spectra for $\Gamma = 0.6$ eV and $\Gamma = 0.02$ eV. Figure 8 shows the results for $\mathbf{n}=(111)$, (110) and (100) , $\hbar\omega_1 = \epsilon_{\min} - \epsilon_c$, where ϵ_{\min} is the minimum energy of conduction-bands. From figure 8, we can see following facts. In the case of realistic value of Γ , more channels than the case of sufficiently small value of Γ are opened to excite an electron with different momenta in the conduction band. We need to sum up each contribution. As a result, spectral components of band-to-band transitions become broader than the case of smaller value of Γ . Although spectral components moves with varying \mathbf{n} , we cannot find the clear correspondence between the peaks of spectral components and the valence bands. Moreover, the peak structure of spectral components are smeared out in RIXS spectrum because the spectral components are broad enough to overlap each other. Therefore, we cannot find the clear correspondence between the peaks of RIXS spectra and the dispersion of valence bands. We also confirm that the anisotropy disappears from RIXS spectra for $\Gamma \geq 1.5$ eV as is the case of RIXS at the K edge of Ge⁴(whose results are not presented in this paper). Summarizing this subsection, we conclude that the value of core-level width of Si is barely small to have anisotropy in RIXS but not small enough to determine the band structure from RIXS spectra.

4. Concluding Remarks

We have investigated theoretically the RIXS at K edge of Si with varying transferred-momenta, incident-photon energy and incident-photon polarization. We have confirmed theoretically the anisotropy of RIXS and have provided a quantitative explanation of a experiment on RIXS at the K edge of Si performed by Ma *et. al.*⁶ We have clarified the implication of the spectral shape. To have an anisotropy in RIXS, the sizable momentum transfer and core-level width smaller than conduction-bandwidth are required. The photon energy is required to obtain sizable momentum transfer but corresponding core-level widths are usually large. Therefore, it is difficult to satisfy the requirement of the sizable momentum transfer and small core-level width. In the case of RIXS at the K edge of Si, we have pointed out that the value of core-level width of Si is barely small to have anisotropy in RIXS but not small enough to determine the band structure from RIXS spectra.

Acknowledgment

Authors greatly thank to Prof. N. Hamada for allowing us to use his FLAPW code. One of the authors (Y.N.) also thanks to Dr. A. Agui for helpful discussion.

References

- 1) M. Z. Hasan, E. D. Isaacs, Z.-X. Shen, L. L. Miller, K. Tsutsui, T. Tohyama, and S. Maekawa, *Science* **288** (2000) 1811.
- 2) Y. J. Kim, J. P. Hill, C. A. Burns, S. Wakimoto, R. J. Birgeneau, D. Casa, T. Gog, and C. T. Venkataraman, *Phys. Rev. Lett.* **89** (2002), 177003.
- 3) T. Inami, T. Fukuda, J. Mizuki, S. Ishihara, H. Kondo, H. Nakao, T. Matsumura, K. Hirota, Y. Murakami, S. Maekawa, and Y. Endoh, *Phys. Rev. B* **67** (2003) 045108.
- 4) Y. Nisikawa, M. Usuda, J. Igarashi, H. Shoji, and T. Iwazumi, *J. Phys. Soc. Jpn.* **73** (2004) 970.
- 5) Y. Ma, *Phys. Rev. B* **49** (1994) 5799.
- 6) Y. Ma, K. E. Miyano, P. L. Cowan, Y. Aglitzkiy, and B. A. Karlin, *Phys. Rev. Lett.* **74** (1995) 478.
- 7) S. H. Vosko, L. Wilk and M. Nusair, *Can. J. Phys.* **58** (1980) 1200.
- 8) J. H. Scofield, *Phys. Rev.* **179** (1969) 9.
- 9) V. O. Kostroun, M. H. Chen, and B. Crasemann, *Phys. Rev. A* **3** (1971) 533.

Fig. 1. Energy vs. momentum relation of Si calculated by the FLAPW method in the LDA scheme. The energy band is labeled by attached numbers for decomposing the RIXS spectra into each contribution of band-to-band transitions

Fig. 2. Setup for scattering: geometrical relations between \mathbf{q}_1 , \mathbf{q}_2 and sample crystal of Si.

Fig. 3. RIXS spectra obtained by (a)experiment[6] and (b)theory. The RIXS spectra were normalized to have same area. The anisotropy of the RIXS can be found in the spectra.

Fig. 4. Calculated RIXS spectra for $\mathbf{n}=(111)$ with varying incident-photon energy between 1840.0 eV and 1841.2 eV. The characteristic three peaks A, B and C in RIXS spectra is found only in the narrow energy region between 1840.2 eV and 1840.8 eV.

Fig. 5. Calculated RIXS spectra for $\hbar\omega_1 = 1842.5$ eV with varying $\mathbf{n}=(111)$, (110) , and (100) . The anisotropy of RIXS almost disappear from the spectra

Fig. 6. Calculated RIXS spectra with varying incident-photon polarization. The low energy-loss parts of spectra for $\mathbf{n}=(100)$ change by varying the incident-photon polarization.

Fig. 7. The RIXS spectra for $\hbar\omega_1 = 1840.8$ eV, $\mathbf{n}=(111)$, (110) , and (100) are decomposed into each contribution of band-to-band transitions specified by band indices defined in the figure. 1.

Fig. 8. The RIXS spectra for realistic value of core-level width ($\Gamma = 0.6$ eV) in comparison with the RIXS spectra for sufficiently small value of core-level width ($\Gamma = 0.02$ eV). The spectral components of band-to-band transitions for each RIXS spectrum are also shown in this figure. The dash-dot lines are to guide the eye to the peak positions of the RIXS spectra for $\Gamma = 0.02$ eV.

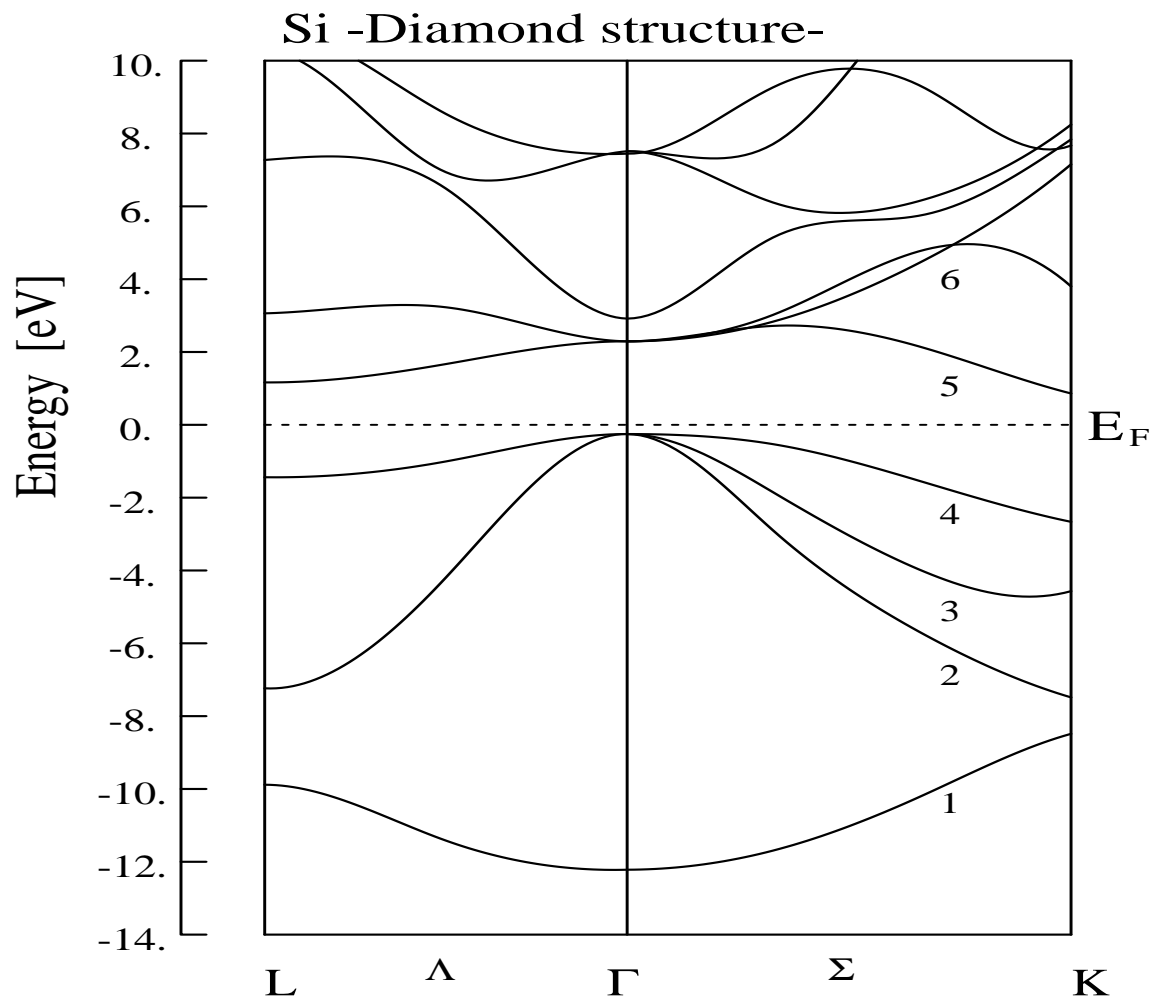


Fig. 1. Y.Nisikawa et al.

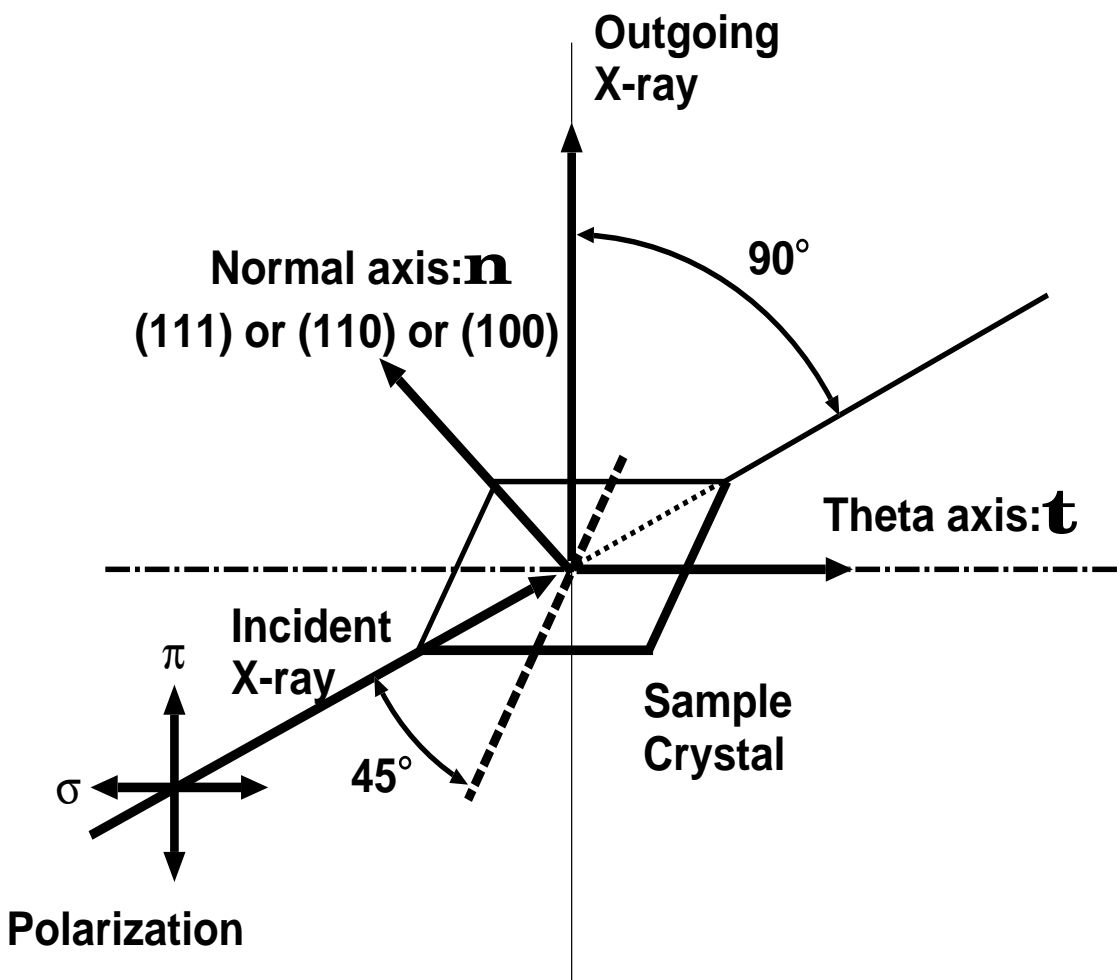


Fig. 2. Y.Nisikawa et al.

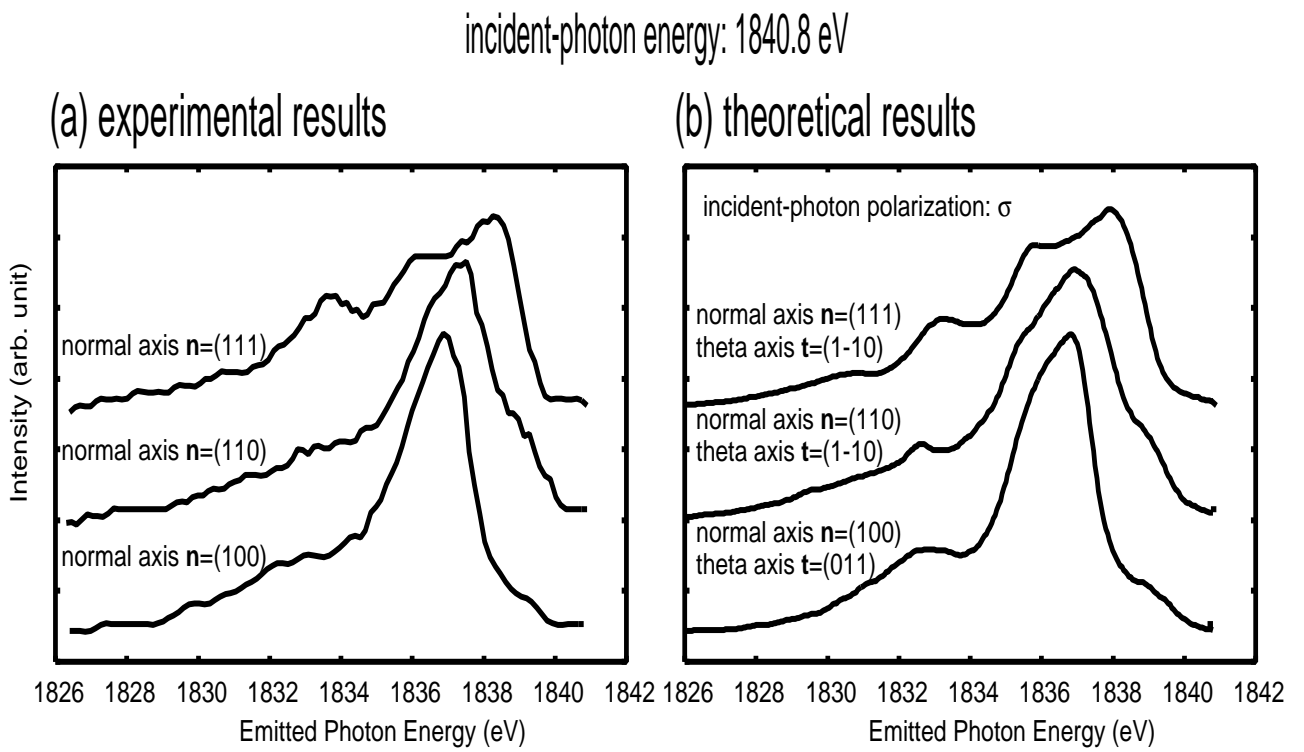


Fig. 3. Y.Nisikawa et al.

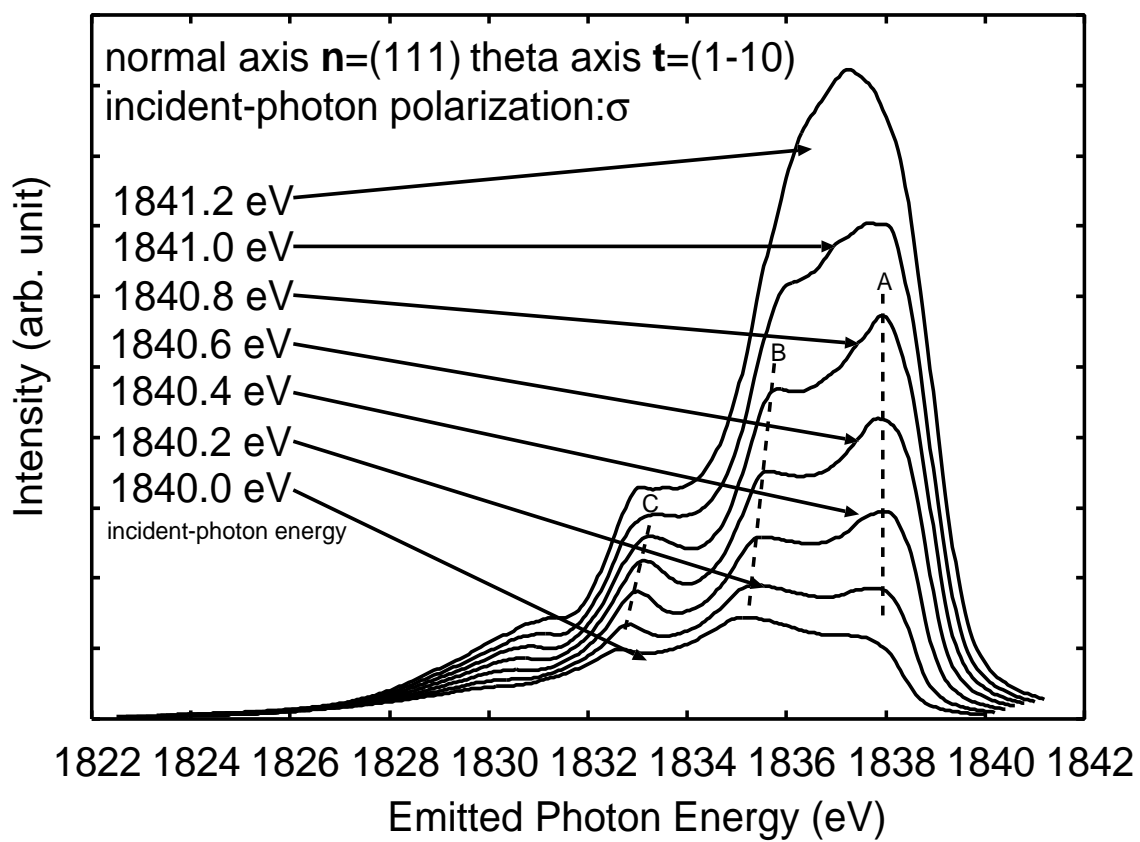


Fig. 4. Y.Nisikawa et al.

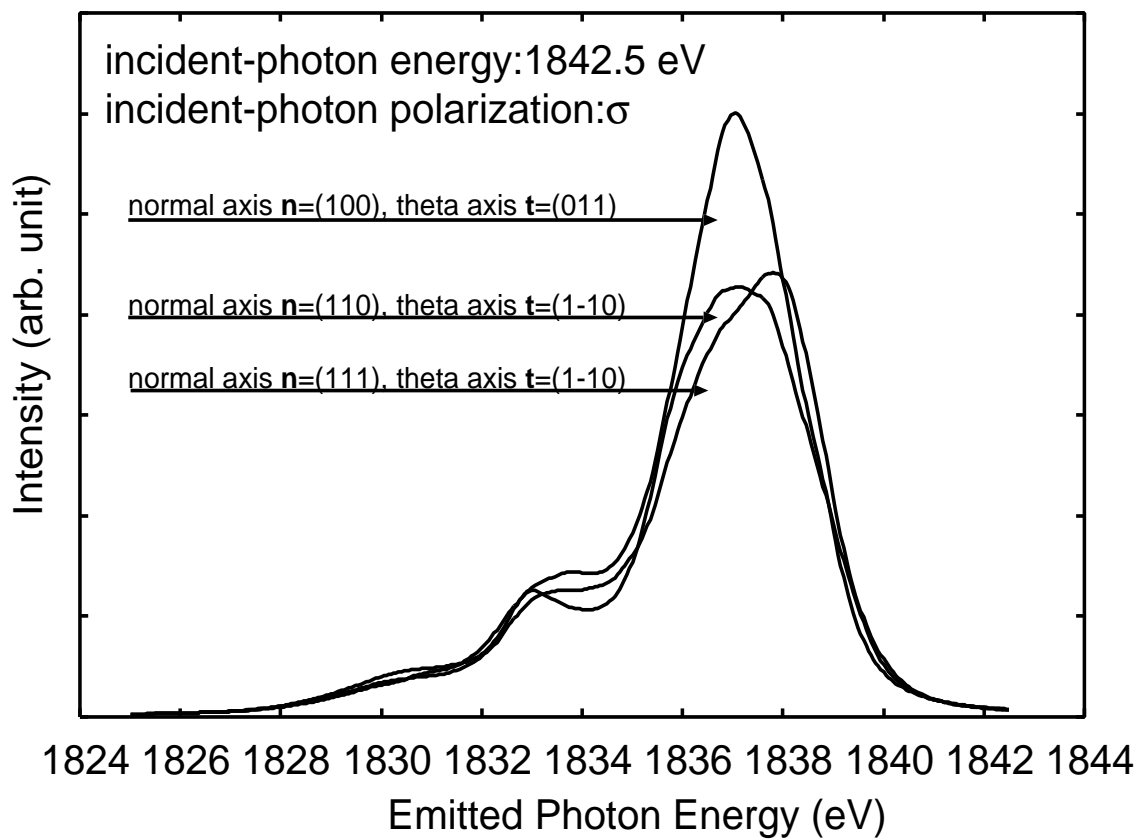


Fig. 5. Y.Nisikawa et al.

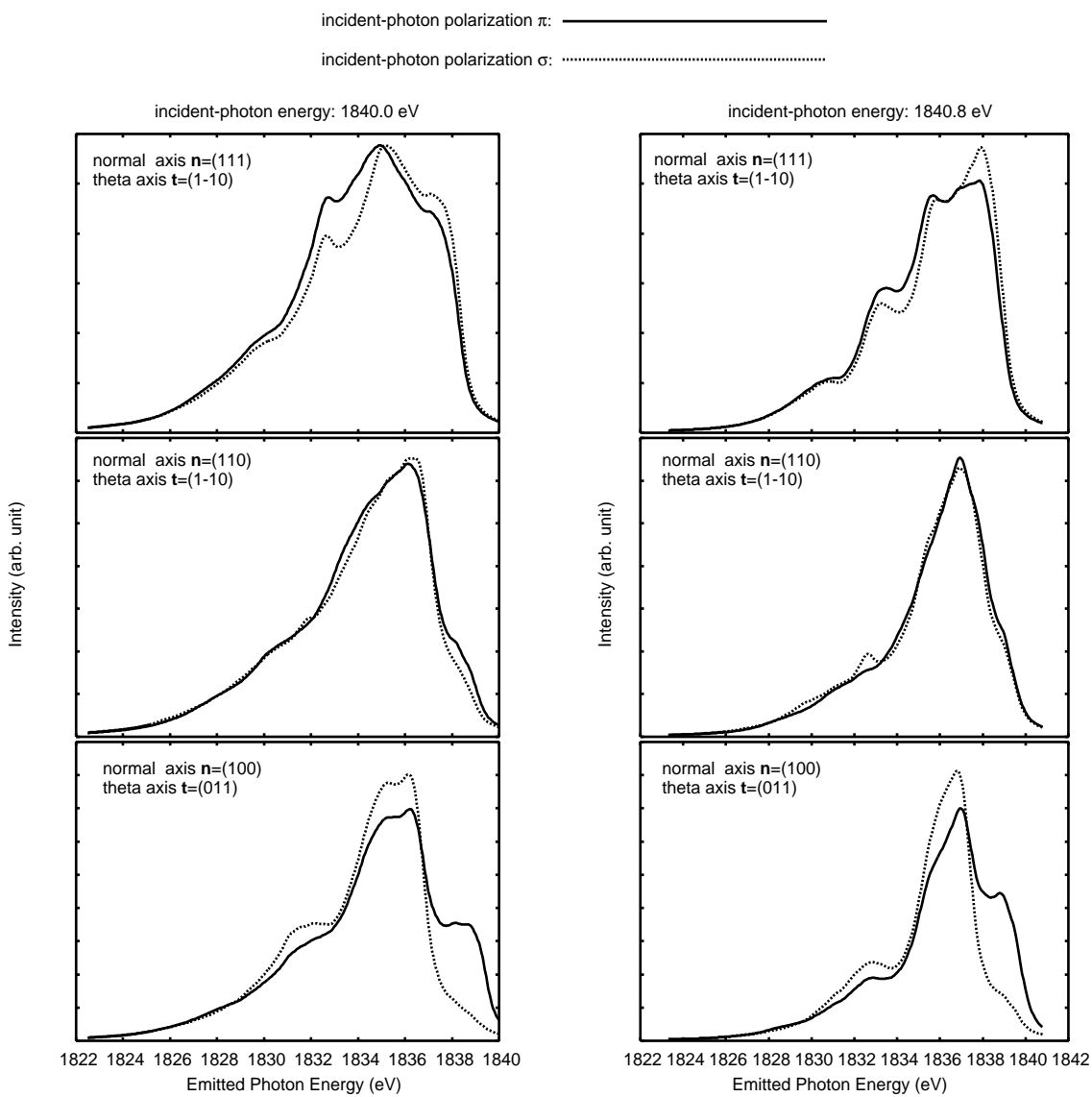


Fig. 6. Y.Nisikawa et al.

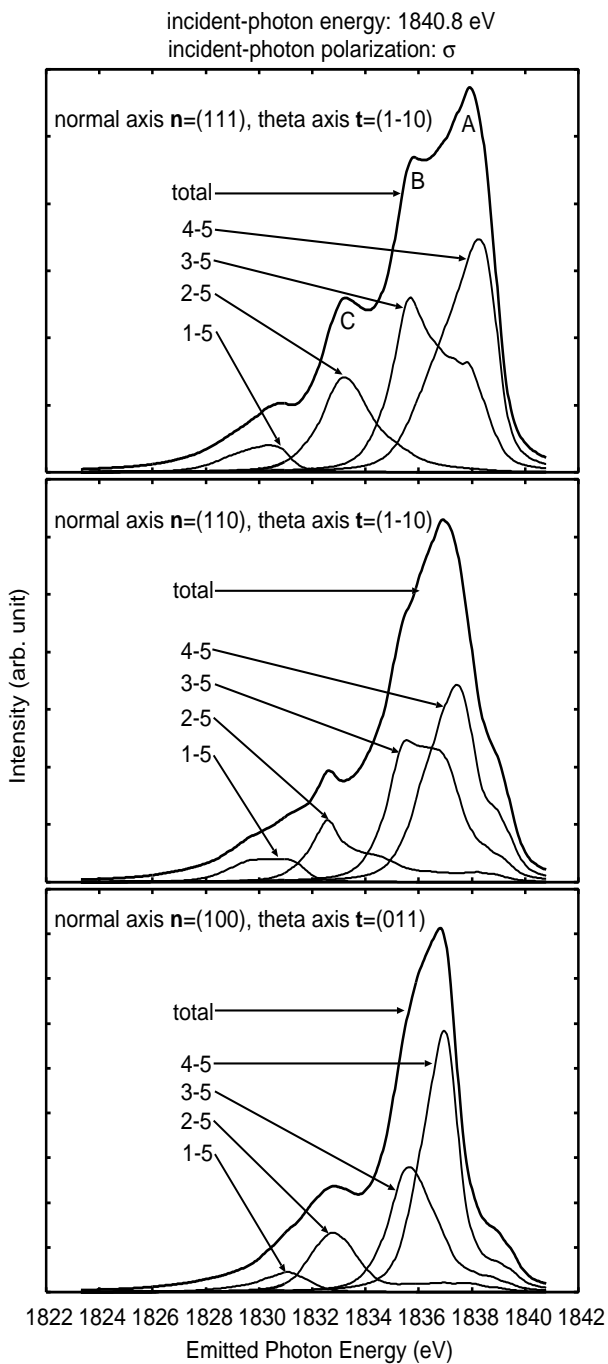


Fig. 7. Y.Nisikawa et al.

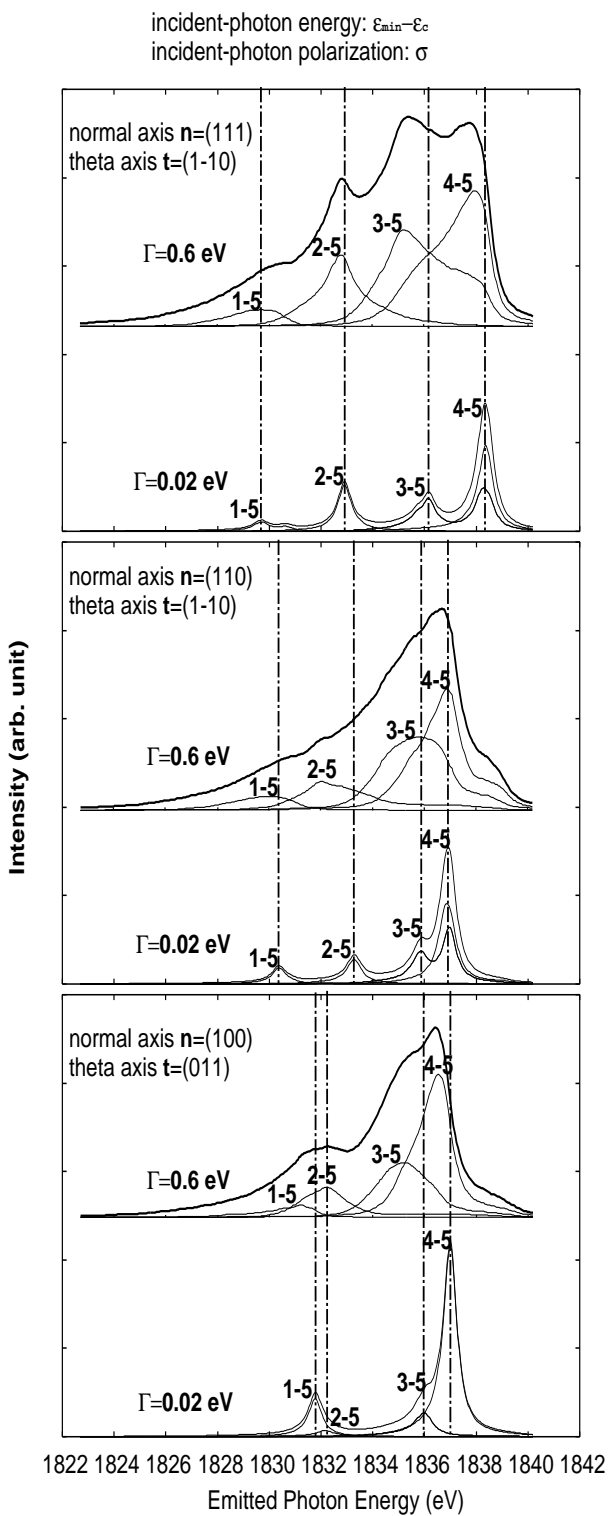


Fig. 8. Y.Nisikawa et al.